Nanotechnology Perceptions
ISSN 1660-6795
www.nano-ntp.com

Experimental Investigation to Evaluate Mechanical Properties on Nano Graphene Added CFRP Laminates

V. Nikil Murthy[1], Dr. Ashwin C Gowda[2], Dr. Santhosh N[3], Dr. Dhanunjaya Munthala[4], Dileep B. P[5]

[1]Research scholar, Department of Mechanical Engineering, VTU Regional centre, Muddenahalli, chikballapur, Bangalore. murthy362@gmail.com
[2]Department of Mechanical Engineering, VTU Regional centre, Muddenahalli, chikballapur, Bangalore. acgmech@gmail.com
[3]Department of Mechanical Engineering, MVJ College of Engineering, Near ITPB, Whitefield, Channasandra Main Road, Bangalore, dr.santhosh@mvjce.edu.in
[4]Institute of Research and Development (IRD), Suranaree University of Technology, Thailand, dhanuphy@gmail.com
[5]Department of Mechanical Engineering, Amrita School of Engineering, Bengaluru, Amrita Vishwa Vidyapeetham, India, bp_dileep@blr.amrita.edu

Polymers are regularly supported by different estimated fillers to lighten a portion of the constraints of the polymers. The use of nanoscale fillers to work on mechanical and thermal properties of polymers have prompted to an extreme option for the conventional polymer composites. Their high strength-to-weight ratio, excellent mechanical properties, and resistance to corrosion make them ideal for use in creating lightweight and durable structures. The present work mainly focused on the carbon fibre(CFRP) added with Graphene filler with 3mm thickness and a layer thickness of 0.5mm in vacuum impingement moulding process with vacuum bagging at different pressures directions , number of layers and curing temperatures. Graphene Nano particles taken as filler content of 2% which has been done previously as pilot experiments and form literature. The design of experiments selected from Taguchi L9 orthogonal array to prepare samples. A three factorial study from Taguchi has been optimized to check the best parameters for improved mechanical properties in the composite. The direction of injection is taken as top, and diagonal as well as pressure 20 bar, 25 bar and 30 bar with curing temperatures after lamination is 60, 80 and 100℃.

Keywords: CFRP, Nano graphene, Vacuum impinging, Curing temperatures,

Mechanical properties, Taguchi, Optimization.

1. Introduction

Industrial evolution has led to a huge demand for novel materials which have high strength and toughness, wide availability and are less costly [1] More importantly, a high strength-to-low weight ratio is an ideal property for many structural applications such as aircraft and automotive [2,3]. Polymer composites are highly adapted materials for this purpose [4]. Recently, an immense interest has grown in finding new fillers and techniques to further improve the mechanical and functional properties of these composites The major consumption of fiber-reinforced polymer composites is commonly observed in aircraft sectors owing to their unique characteristics of high strength and low weight and excellent fatigue strength [5][6]. In the modern age, the failure of many structural materials such as aircraft materials often caused by reinforcing structures that work in fracture toughness mode, comes with many problems [7]. To address this issue, researchers are concentrating on high-performance glass and carbon fiber epoxy-based composites [8]. Despite meeting the overall needs of the aircraft industry, the critical fracture toughness attribute is insufficient due to epoxy's extensive cross-linking. The aircraft may be subjected to a variety of low and high-velocity impacts as a result of crashes and luggage drops, altitude variations, and bird strikes during take-off [8][9]. As a result, aircraft structures may suffer some serious damage, with the possibility of cracks developing . Among all the factors, lightning strikes have a major impact on the performance of fiber-reinforced composites [10]. The use of multifunctional nanocomposites, which improve both electrical conductivity and interlaminar mechanical properties, is one strategy to mitigate this issue. For instance, woven composite's performance may improve through changing toughness within and away from interlaminar resin pockets [11]. The failure mechanism of fiber composites is still difficult to grasp For instance, out-of-plane compression was related to the failure of shear fibers and the rupture of fiber bundles, whereas interfacial debonding led to in-plane compression fracture. The dispersion and amount of nanoparticles, curing conditions, and interfacial adhesion of composites are among the variables that influence their mechanical properties [12][13][14]. Nanomaterials such as graphene and its variants along with carbon nanotubes (CNTs) have been gaining tremendous attraction, due to their unique characteristics, including their functions, molecular structure, and spreading capacity [15]. These two nanofillers are considered to be the next generation aeroplane materials. The aerospace industry is looking into ways to enhance the mechanical properties of epoxy composites. Graphene is the strongest and thinnest two-dimensional (2D) material that humanity has ever discovered [16]. Due to its distinct attributes, the creation of graphene opened the door to becoming a potential material with significant engineering applicability [17][18]. the properties of graphene/polymer composites and their various emerging applications. Moreover, in-plane strong covalent bonds in graphene material, significantly affect the load, electron, and phonon transfer behavior of the nanocomposites Graphene or other 2D material nanosheets exhibit a strong adhesion effect or mechanical interlocking with epoxy due to the lamellar structure and result in improved mechanical as well thermal properties of nanocomposites [22][23]. Additionally, graphene also improves the toughness of epoxy resins [19] [20] [21] . Carbon-fibre-reinforced polymer (CFRP) composites have been

investigated and utilized extensively, with their key advantages including lightweight, high specific strength and stiffness, good corrosion resistance, etc [24]. The superb properties of CFRP composites enable them to be employed for high-end applications, such as aerospace and automotive [25]. After decades of research, the manufacturing technology of CFRP composites has been improved with more economical production, which paves the route for its applications in oil and gas industry

1.1 Significance of work

Conventional methods for NANO graphene addition to CFRP leads to wastage of materials like hand lay up methods and more over the deposition of material will not spread evenly. To avoid such factors in the CFRP laminates Vacuum impingement method considered for the present work. The variation in mechanical properties compared with the conventional laminates to check the differentiation, furture work to check viscoelastic properties can compare for better optimal parameters during fabrication procedure.

2. Methodology

Impinging is a method of using air nozzles to create a vacuum on the surface of a composite material, which then sucks in the laminate and adheres it to the substrate. This creates a strong bond between the laminate and the substrate, which is essential for many applications. Adding Nano graphene to Carbon Fiber Reinforced Polymers (CFRP) through a vacuum impinging method is a promising approach to enhance the material's mechanical, thermal, and electrical properties. Graphene, a single layer of carbon atoms arranged in a hexagonal lattice, possesses extraordinary properties: High thermal conductivity, excellent electrical conductivity, remarkable mechanical strength. When it added to CFRP it can improve mechanical strength and stiffness, enhance thermal conductivity and dissipation, improve electrical conductivity, enhance resistance to fatigue and impact damage.

2.1 Vacuum Impinging: A Precise Technique

Vacuum impinging is a manufacturing process that involves applying a high-velocity stream of resin to a fiber reinforcement under vacuum conditions. This technique offers several advantages for incorporating Nano graphene into CFRP:

- Uniform Dispersion: The high-velocity impact helps to disperse the Nano graphene particles evenly throughout the resin matrix, ensuring optimal performance.
- Improved Interfacial Bonding: The vacuum environment aids in removing air bubbles and voids, leading to enhanced interfacial bonding between the graphene nanoparticles and the carbon fibers.
- Enhanced Penetration: The high-velocity impact can help the nano graphene particles penetrate deeper into the fiber matrix, improving the overall properties of the composite. The process technique shown in the figure1.

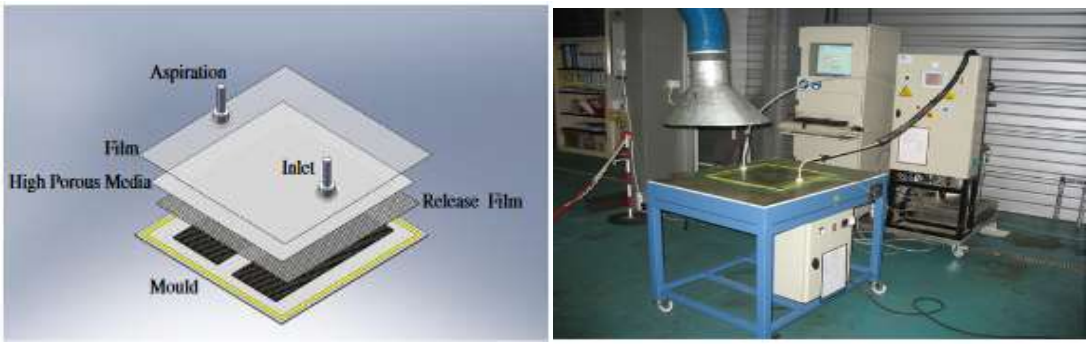

Figure1: Vacuum impinging process

The initial leakage has been checked for 5-10 minutes by generating the vacuum inside the assembly. The inlet valve has been opened after confirming air tight setup and at the same time vacuum has been applied through the vacuum pump. The resin has been sucked through PVC pipe and slowly pass through layers of carbon fabric.

2.2 Materials for laminate preparation

Matrix: Epoxy-resin LY-556 (Bisphenol - A), Aradur

Hardner : Araldite HY951

Nano fillers: Grephene Nano particles

Reinforcement : Carbon fiber

2.2.1 Properties of NANO graphene

The incorporation of NANO graphene can significantly enhance both tensile and flexural strength due to its exceptional mechanical properties. Its high surface area and strong bonding capabilities contribute to improved load transfer and reinforcement in composite materials.The properties of Nano powder of graphene given in the following table1.

Table1: Properties of graphene NANO particles

Density	Melting point	Boiling point	Purity	Average particle size	Specific surface area	Appearance
1.8gm/cm^3	3550^{0}C	4270^{0}C	99%	<50nm	100M^2/gm	Black

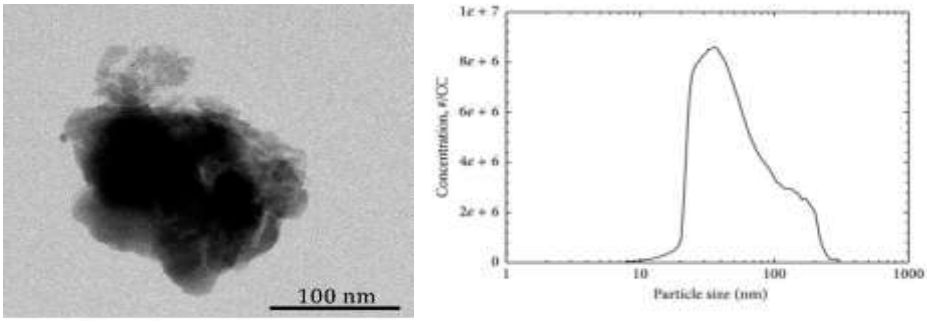

Figure2: Graphene nano particle size representation

Taguchi L9 orthogonal array used to prepare design of experiments with variable parameters to predict optimal parameters on the basis of tensile and flexural strengths.

Table:2 L9 3^3 orthogonal array

	No. of Layers	Pressure (Bar)	Curing Temperatures
1	1 (3L)	1 (20)	1 (60)
2	1(3L)	2 (25)	2 (80)
3	1(3L)	3 (30)	3 (100)
4	2 (4L)	1 (20)	2 (80)
5	2 (4L)	2 (25)	3 (100)
6	2 (4L)	3 (30)	1 (60)
7	3 (6L)	1 (20)	3 (100)
8	3(6L)	2 (25)	1 (60)
9	3(6L)	3 (30)	2 (80)

Two orthogonal array of total 18 samples taken 9+9 comparison with tensile and flexural properties. CFRP laminates prepared at a temperature of 150^0C and the curing temperatures are varied.

2.3 Samples after fabrication:

Prepared samples from two injected directions one is from top and second from diagonal with vacuum impinging method. The tested samples after testing with layer formation shown in figure 3.

Figure 3: Tested samples after fabrication

4. Results and discussions

This study was conducted to assess the mechanical properties of CFRP with graphene filler epoxy laminates. The results of the study showed that the vacuum impinging method had improved mechanical properties compared to conventional CFRP epoxy laminates, and that the process are reliable and it was more resistant to impact damage. The results obtained for tensile and flexural has been given in table3 for top impinging

Table 3: Result's for top impinging direction for Epoxy/ Nano

	No. of Layers	Pressure (Bar)	Curing Temperatures	Tensile strength (UTS) (MPa)	Flexural strength (MPa)
1	3L	20	60	248	125
2	3L	25	80	256	129
3	3L	30	100	252	119
4	4L	20	80	267	134
5	4L	25	100	254	126
6	4L	30	60	259	128
7	6L	20	100	256	125

8	6L	25	60	266	131
9	6L	30	80	279	133

Table 4: Result's for top impinging direction for Epoxy/ Nano

	No. of Layers	Pressure (Bar)	Curing Temperatures	Tensile strength (UTS) (MPa)	Flexural strength (MPa)
1	3L	20	60	269.1	133.4
2	3L	25	80	277.8	137.7
3	3L	30	100	273.4	127.0
4	4L	20	80	289.7	143.1
5	4L	25	100	275.6	134.5
6	4L	30	60	281.0	136.7
7	6L	20	100	277.8	133.5
8	6L	25	60	288.6	139.9
9	6L	30	80	302.7	142.0

4.1 Taguchi prediction for optimal parameters

In Taguchi's approach, the aim is to find a suitable combination of parameters that minimizes the mean of the responses. This is done by minimizing the signal-to-noise ratio (SNR). The SNR is calculated by dividing the standard deviation of the response by the difference between the mean of the response and the ideal response. Taguchi's method is a Design of Experiment (DOE) technique used to identify optimal parameters by analyzing the relationship between the response variables and the parameters. This method can be used to gain insight into how changes in the parameters affect the response variables, which can then be used to make predictions about how changes in one parameter will affect the other parameters.

4.2 Taguchi Analysis: TS, FS versus A, B, C

Table 5:Response Table for Signal to Noise Ratios

	Signal to Noise Ratios				Means		
Level	A	B	C		A	B	C
1	43.95	44.19	44.19		188.2	192.5	192.8
2	44.28	44.24	44.47		194.7	193.7	199.7
3	44.34	44.15	43.91		198.3	195.0	188.7
Delta	0.39	0.09	0.56		10.2	2.5	11.0
Rank	2	3	1		2	3	1
	Analysis: Larger is better						

The above table represents Tensile and flexural strength relation after graphene addition. From the above table 5, responses observed for S/N ratio and means the most effective parameter is 'C' that , curing temperature followed by parameter A I.e., number of layers.

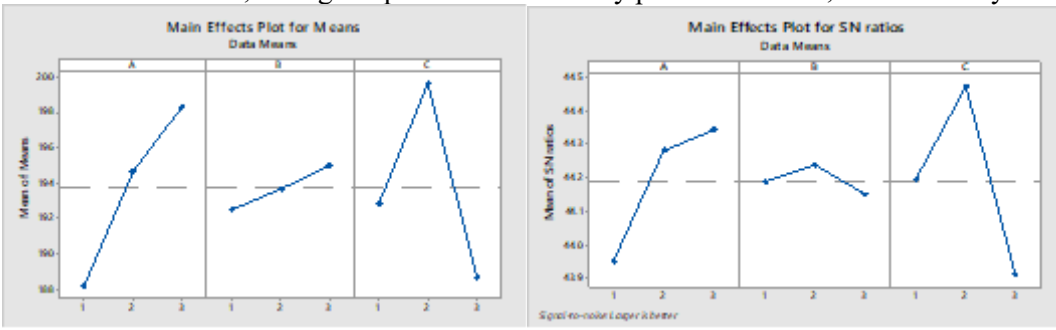

Figure 4: Mean plot and S/N plot

By observing figure 4, for parameters A,B and C Four layers with 25 Bar pressure and

curing temperature of 60^0 C are the mean parameters effectively imposed on Tensile and Flexural Strength.

Table 6:Estimated Model Coefficients for St.Devs.

Term	Coef	SE Coef	T	P
Constant	93.2595	0.8315	112.161	0.000
A 1	-2.9856	1.1759	-2.539	0.126
A 2	-0.8642	1.1759	-0.735	0.539
B 1	-2.0428	1.1759	-1.737	0.224
B 2	-1.3356	1.1759	-1.136	0.374
C 1	-1.5713	1.1759	-1.336	0.313
C 2	2.4356	1.1759	2.071	0.174
Model Summary		S	R-Sq	R-Sq(adj)
		2.4944	92.48%	69.91%

From the above table 6 the value deviations mostly observed in the No. of layers with an accuracy of 92.48% of the DOE model selected followed by the pressure. Least deviation found in curing temperatures.

Table 7: Analysis of Variance for Standard Deviation

Source	DF	Seq SS	Adj SS	Adj MS	F	P
A	2	73.44	73.44	36.722	5.90	0.145
B	2	52.11	52.11	26.056	4.19	0.193
C	2	27.44	27.44	13.722	2.21	0.312
Residual Error	2	12.44	12.44	6.222		
Total	8	165.44				

By observing table 7 the most significant factor is No. of layers followed by the input pressure with a 'F' value of 5.9 and 4.19 respectively.

Table 8: Response Table for Standard Deviations

Level	A	B	C
1	90.27	91.22	91.69
2	92.40	91.92	95.70
3	97.11	96.64	92.40
Delta	6.84	5.42	4.01
Rank	1	2	3

By observing response table for standard deviation part in table 8 the effective parameters are No. of Layers followed by the input pressure as shown in ranking 1,2 and 3. The deviation plot showing that strength increases with number of layers from 4 to 6 the deviation increased more followed by injected pressure and curing temperature to 80^0C re

curing temperature after laminating.

Table 9: Taguchi prediction for Optimal Parameters

	No. of Layers	Pressure (Bar)	Curing Temperatures	S/N Ratio	Mean	StDev	Ln(StDev)	Rank
1	3L	20	60	-38.7732	186.056	86.6599	4.46393	9
2	3L	25	80	-39.2054	194.056	91.3739	4.51368	8
3	3L	30	100	-39.3417	184.389	92.7881	4.52938	5
4	4L	20	80	-39.3417	199.389	92.7881	4.52938	2
5	4L	25	100	-39.4747	195.056	94.2023	4.54469	7
6	4L	30	60	-39.4747	195.056	94.2023	4.54469	4
7	6L	20	100	-39.4747	192.056	94.2023	4.54469	6
8	6L	25	60	-39.4714	197.389	94.2023	4.54431	3
9	6L	30	80	-40.2622	205.556	102.923	4.63536	1

By observing Taguchi prediction for Optimal Parameters in the table 9 for the mean and standard deviation part the effective parameters are No. of Layers followed by the input pressure and temperature by ranking 1 to 9.

4.2.1 Regression Analysis: TS versus A, B

Table 10: Analysis of Variance

Source	DF	Adj SS	Adj MS	F-Value	P-Value	Model Summary			
Regression	2	397.6	198.83	3.68	0.091	S	R-sq	R-sq(adj)	R-sq(pred)
A	1	337.5	337.50	6.24	0.047	7.35225	55.08%	40.10%	0.00%
B	1	60.17	60.17	1.11	0.332				
Error	6	324.3	54.06						
Total	8	722.0							

From the above table 10 the Regression Analysis of TS versus A, B. The most effective Parameter is A with an F value of 6.24. The regression coefficient table11 the tensile strength depends mostly on layers with a T value of 2.50.

Table 11: Regression Coefficients

Term	Coef	SE Coef	T-Value	P-Value	VIF
Constant	238.33	8.84	26.97	0.000	
A	7.50	3.00	2.50	0.047	1.00
B	3.17	3.00	1.06	0.332	1.00
Regression Equation			TS	=	238.33 + 7.50 A + 3.17 B

4.2.2 Regression Analysis: FS versus A, B

Regression analysis of the two factors number of layers and injected pressures the variance table 12 the effective parameter is number of layers with a F value of 2.0 while the injection pressure have low significance with 0.2.

Table 12: Analysis of Variance

Source	DF	Adj SS	Adj MS	F-Value	P-Value
Regression	2	45.333	22.667	1.06	0.403
A	1	42.667	42.667	2.00	0.207
B	1	2.667	2.667	0.12	0.736
Error	6	128.222	21.370		
Total	8	173.556			

The regression coefficients table 13 also indicating that a higher T value of 1.41 found with regular deviation in P value 0.207, The constant value also added with number of layers.

Table 13: Regression Coefficients

Term	Coef	SE Coef	T-Value	P-Value	VIF
Constant	123.78	5.56	22.28	0.000	
A	2.67	1.89	1.41	0.207	1.00
B	-0.67	1.89	-0.35	0.736	1.00
Regression Equation			FS	=	123.78 + 2.67 A - 0.67 B

Regression Analysis of TS versus A, C. The most effective parameter is 'A' i.e., No. of layers as given in the table 14. For tensile the curing temperature is not much effective factor as the f value is 0.33.

Table 14: Regression Analysis: TS versus A, C Analysis of Variance

Source	DF	Adj SS	Adj MS	F-Value	P-Value
Regression	2	357.67	178.83	2.95	0.128
A	1	337.50	337.50	5.56	0.056
C	1	20.17	20.17	0.33	0.585
Error	6	364.33	60.72		
Total	8	722.00			

The regression coefficients for Flexural strength the curing temperature also resembles with a p value of 0.585 as shown in table 15.

Table15: Regression Coefficients for FS

Term	Coef	SE Coef	T-Value	P-Value	VIF
Constant	248.33	9.37	26.52	0.000	
A	7.50	3.18	2.36	0.056	1.00
C	-1.83	3.18	-0.58	0.585	1.00
Regression Equation			TS	=	248.33 + 7.50 A - 1.83 C

Table 16: Regression Analysis: FS versus A, C Analysis of Variance

Source	DF	Adj SS	Adj MS	F-Value	P-Value
Regression	2	75.33	37.67	2.30	0.181
A	1	42.67	42.67	2.61	0.158
C	1	32.67	32.67	2.00	0.207
Error	6	98.22	16.37		
Total	8	173.56			

Regression Analysis of FS versus A, C from the above table 16 the most effective parameter is 'A' i.e., No. of layers followed with similar significance in curing temperatures with a F value of 2.61 and 2.0 and P value of 1.58 and 0.207. The regression coefficients indicate that after the curing temperature 80^0C the fluxeral strength decreased with increase of temperature with a negative value shown in the table 17.

Table 17: Regression coefficients for FS

Term	Coef	SE Coef	T-Value	P-Value	VIF
Constant	127.11	4.86	26.14	0.000	
A	2.67	1.65	1.61	0.158	1.00
C	-2.33	1.65	-1.41	0.207	1.00
Regression Equation			FS	=	127.11 + 2.67 A - 2.33 C

By considering all the factors for regression the tensile strength influenced by number of layers followed by injection pressure from the diagonal axis with F values 2.23 and 0.79 as given in the table 18. Tensile strength coefficients from the table 19 by keeping no of layers constant the other two parameters B and C that is injected pressure and curing temperatures , B is the effective factor with positive values in T and P values 0.89 and 0.424 respectively.

Table 18: Analysis of Variance (Regression Analysis: TS versus B, C, A Method)

Source	DF	Adj SS	Adj MS	F-Value	P-Value
Regression	4	418.33	104.58	1.38	0.382
A	2	338.00	169.00	2.23	0.224
C	1	20.17	20.17	0.27	0.633
B	1	60.17	60.17	0.79	0.424
Error	4	303.67	75.92		
Total	8	722.00			

Table 19: Tensile strength Coefficients

Term	Coef	SE Coef	T-Value	P-Value	VIF	Regression Equation				
Constant	249.3	11.2	22.17	0.000						
A										
2	8.00	7.11	1.12	0.324	1.33		A			
3	15.00	7.11	2.11	0.103	1.33		1	TS	=	249.3 - 1.83 C + 3.17 B
C	-1.83	3.56	-0.52	0.633	1.00		2	TS	=	257.3 - 1.83 C + 3.17 B
B	3.17	3.56	0.89	0.424	1.00		3	TS	=	264.3 - 1.83 C + 3.17 B

Table 20: Analysis of Variance (Regression Analysis: FS versus B, C, A Method)

Source	DF	Adj SS	Adj MS	F-Value	P-Value
Regression	4	88.889	22.222	1.05	0.482
A	2	53.556	26.778	1.27	0.375
C	1	32.667	32.667	1.54	0.282
B	1	2.667	2.667	0.13	0.741
Error	4	84.667	21.167		
Total	8	173.556			

By considering all the factors for regression the tensile strength influenced by number of layers followed by curing temperature from the diagonal axis with T value 1.42 and P value 0.282 as given in the table 21.

Table 21: Coefficients for FS(Flexural strength)

Term	Coef	SE Coef	T-Value	P-Value	VIF	Regression Equation				
Constant	130.33	5.94	21.94	0.000						
A										
2	5.00	3.76	1.33	0.254	1.33		A			
3	5.33	3.76	1.42	0.229	1.33		1	FS	=	130.33 - 2.33 C - 0.67 B
C	-2.33	1.88	-1.24	0.282	1.00		2	FS	=	135.33 - 2.33 C - 0.67 B
B	-0.67	1.88	-0.35	0.741	1.00		3	FS	=	135.67 - 2.33 C - 0.67 B

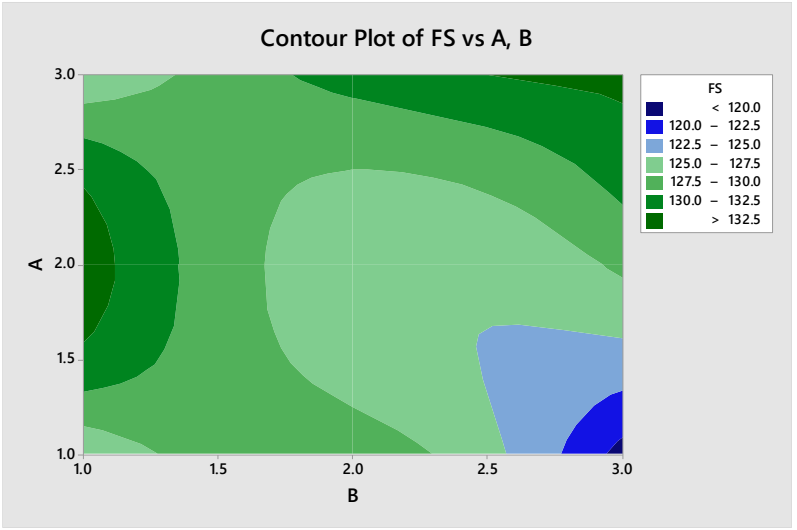

Figure 5: Contour plot of Flexural Strength vs Parameter A,B

The contour plot in figure 5 observed for Flexural strength, most of the experiments by considering the no of layers and injection pressure consideration A is the effective factor and the maximum area covered between strengths observed between 125 to 130

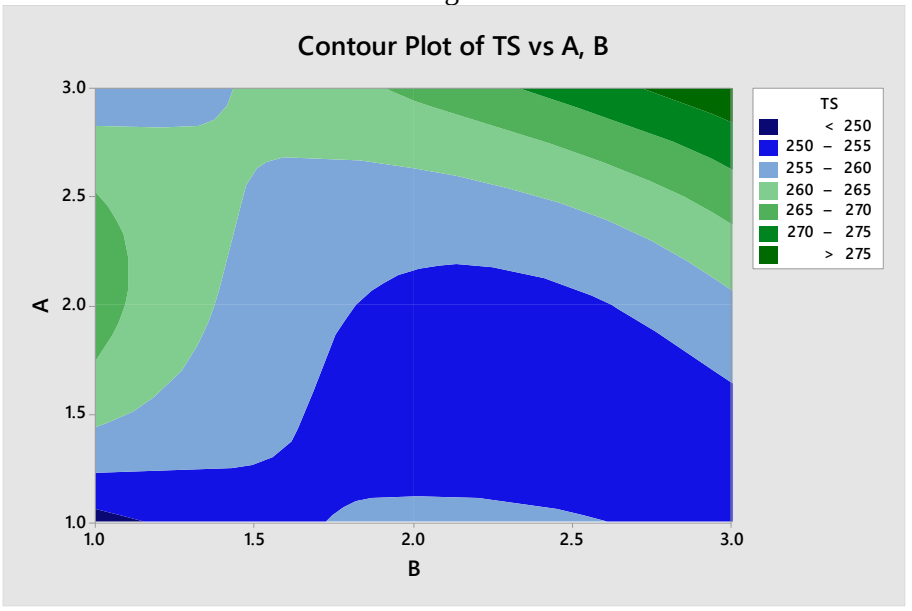

Figure 6: Contour plot of Tensile Strength vs Parameter A,B

In this fig 6 To perspective on the relationship between TS and Parameters A and B. In the bottom-middle region of the plot, where A is near 1.5 and B is between 1.5 and 2.5, the TS values that are the smallest (<250) are clustered. As both A and B are close to 3.0 at the upper right region of the plot, the largest TS values (>275) are located there. This indicates that the TS will also grow as A and B both increase.

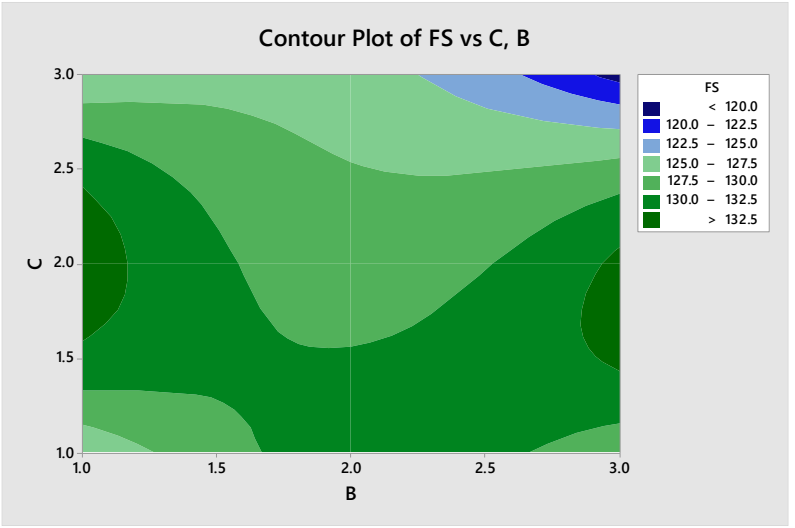

Figure 7: Contour plot of Flexural Strength vs Parameter C,B

From the above figure 7 the variation of Flexural strength observed between 125 to 132, considering the two factors, curing temperature and pressure. According to the contour plot, flexural strength is affected by both the curing temperature and the curing pressure. That being said, the relative importance of each appears to shift depending on the interplay of these variables.

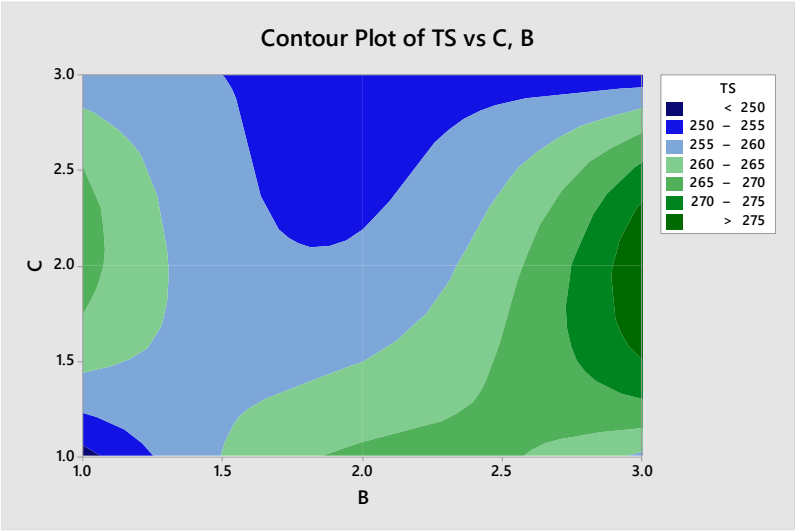

Figure 8: Contour plot of Tensile Strength vs Parameter C,B

From the above figure 8 the variation of Tensile strength observed between 250 to 260 i.e., 50% and 260 to 275 i.e., 50%. considering the two factors, curing temperature and pressure. It is feasible to cure at lower temperatures and pressures to obtain tensile strengths between 250 and 260 GPa. In most cases, it is preferable to cure at higher temperatures and pressures for TS values between 260 and 275.

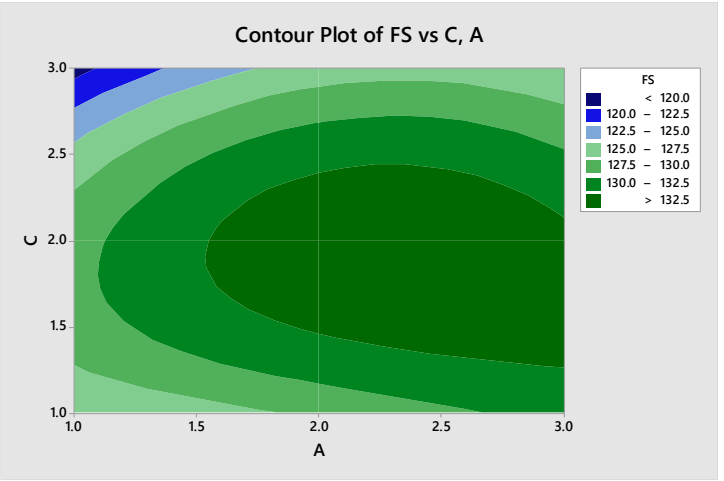

Figure 9: Contour plot of Flexural Strength vs Parameter C, A

The variation in flexural strength is illustrated in Figure 9. It can be observed that a Flexural strength in the range of 125 to 132 can be achieved by either increasing the number of layers or decreasing the curing temperature. However, this graph does not account for other variables, such as processing time and cost, which are essential for determining the optimal combination.

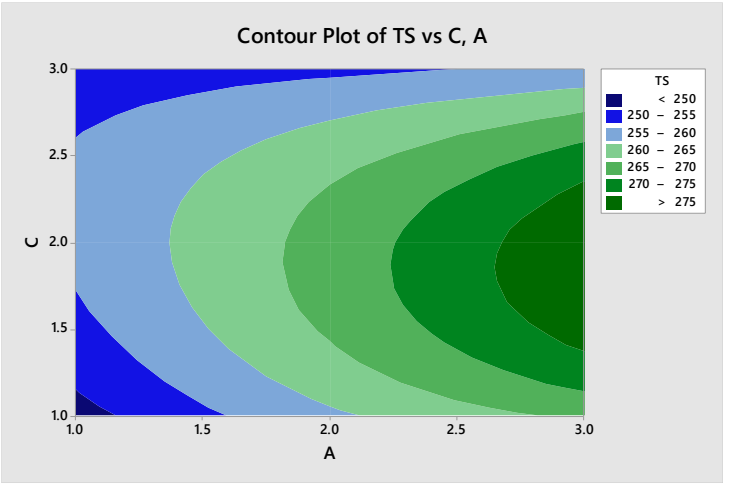

Figure 10: Contour plot of Tensile Strength vs Parameter C, A

The contour plot indicates that tensile strength (TS) values between 250 and 260 are predominantly observed. To help regions achieve these TS values, it is generally more favorable to use lower curing temperatures and fewer layers.

5.Conclusions

Three factors varied with two injection directions and two out put parameters considered for Taguchi prediction. From the above number of layers increases the strength of the laminate with diagonal injection pressure where as curing temperature up to 80^0 given better results, after the increment of temperature the strength decreased for the laminates. The addition of nano Graphene to CFRP laminates using the vacuum impinging method significantly

enhances the mechanical properties of the composites. This integration results in improved tensile strength, increased fracture toughness, and better thermal conductivity. Furthermore, the lightweight nature of nano Graphene contributes to maintaining the overall low weight of the composite material, making it ideal for aerospace and automotive applications.

References

1. Ramesh, V.C. Uvaraja, B.Gnanasundara Jayaraja, P.P. Patil (2022), Fatigue, fracture toughness and DMA of biosilica toughened epoxy with stacked okra fiber and Al 2024-T3 fiber metal laminate composite, Polym. Compos. 43 (9) 6300–6309, https://doi.org/10.1002/pc.26938.
2. Y. Khalid, Z.U. Arif, A. Al Rashid (2021), Investigation of tensile and flexural behavior of green composites along with their impact response at different energies, Int. J. Precis. Eng. Manuf. Technol. , https://doi.org/10.1007/s40684-021- 00385-w.
3. Heggemann, W. Homberg ((2019), Deep drawing of fiber metal laminates for automotive lightweight structures, Compos. Struct. 216 53–57, https:// doi.org/10.1016/j.compstruct.2019.02.047. February
4. Lokesh, T.S.A. Surya Kumari, R. Gopi, G.B. Loganathan (2020), A study on mechanical properties of bamboo fiber reinforced polymer composite, Mater. Today Proc. 22, 897–903, https://doi.org/10.1016/j.matpr.2019.11.100
5. X. Ma, F. Wang, Z. Wang, Y. Li, B. Xu (2021), Thermal dynamic damage of aircraft composite material suffered from lightning channel attachment based on moving mesh method, Compos. Sci. Technol. 214, 109003, https://doi.org/ 10.1016/j.compscitech.2021.109003.
6. X.L. Zhang, J.C. Wang, Q. Xu, Y.Y. Wang, C.Y. Li (2022), Analysis of the openings of aircraft composite laminated wing beam web under shear load, IOP Conf. Ser. Mater. Sci. Eng. 1242 (1) 12044, https://doi.org/10.1088/1757-899X/ 1242/1/012044.
7. G. Kastratovi´ c, A. Grbovi´ c, A. Sedmak, ˇ Z. Boˇ zi´ c, S. Sedmak (2021), Composite material selection for aircraft structures based on experimental and numerical evaluation of mechanical properties, Procedia Struct. Integr. 31, 127–133, https:// doi.org/10.1016/j.prostr.2021.03.021.
8. M.Y. Khalid, Z.U. Arif, W. Ahmed, H. Arshad (2021), Recent trends in recycling and reusing techniques of different plastic polymers and their composite materials, Sustain. Mater. Technol. e00382, https://doi.org/10.1016/J.
9. M.T. Demirci (2022), Investigation of low-velocity impact behavior of aluminum honeycomb composite sandwiches with GNPs doped BFR laminated face-sheets and interfacial adhesive for aircraft structures, Polym. Compos. 43 (8) 5675–5689, https://doi.org/10.1002/pc.26882
10. Z. Feng, K.H. Adolfsson, Y. Xu, H. Fang, M. Hakkarainen, M. Wu (2021), Carbon dot/ polymer nanocomposites: from green synthesis to energy, environmental and biomedical applications, Sustain. Mater. Technol. 29 e00304, https://doi. org/10.1016/J.SUSMAT.2021.E00304.
11. Z Feng, Y Li, C Xin, D Tang, W Xiong, H Zhang (2019), Fabrication of graphene- reinforced nanocomposites with improved fracture toughness in net shape for complex 3D structures via digital light processing, C 5 (2), 25, https://doi. org/10.3390/c5020025
12. P. Govindaraj, et al (2021), Distribution states of graphene in polymer nanocomposites: a review, Compos. Part B Eng. 226, 109353, https://doi.org/10.1016/j. compositesb.2021.109353.
13. B. Fang, D. Chang, Z. Xu, C. Gao (2020), A review on graphene fibers: expectations, advances, and prospects, Adv. Mater. 32 (5), 1902664, https://doi.org/ 10.1002/adma.201902664. February

14. Q. Chen, et al.(2023), An iron phenylphosphinate@graphene oxide nanohybrid enabled flame-retardant, mechanically reinforced, and thermally conductive epoxy nanocomposites, Chem. Eng. J. 454, 140424, https://doi.org/10.1016/j. cej.2022.140424.
15. Du X, Zhou H, Sun W, Liu HY, Zhou G, Zhou H (2017) Graphene/epoxy interleaves for delamination toughening and monitoring of crack damage in carbon fibre/epoxy composite laminates. Compos Sci Technol 140 :123–133.
16. Wang C, Li J, Yu J, Sun S, Li X, Xie F et al (2017) Grafting of size-controlled graphene oxide sheets onto carbon fiber for reinforcement of carbon fiber/epoxy composite interfacial strength. Compos Part A Appl Sci Manuf 101:511–520.
17. Kwon YJ, Kim Y, Jeon H, Cho S, Lee W, Lee JU (2017) Graphene/carbon nanotube hybrid as a multi-functional interfacial reinforcement for carbon fiber-reinforced composites. Compos Part B Eng 122:23–30. https://doi.org/10. 1016/j.compositesb.2017.04.005
18. Eaton MJ, Ayre W, Williams M, Pullin R, Evans SL (2014) Nano-reinforcement of resin infused carbon fibre laminates reinforced using carbon nano-tubes and graphene. In: 16th Int Conf Exp Mech. Cambridge (UK). https://doi.org/10.13 140/2.1.1006.3368.
19. Papageorgiou DG, Kinloch IA, Young RJ (2017) Mechanical properties of graphene and graphene-based nanocomposites. Prog Mater Sci 90:75–127. https://doi.org/10.1016/j.pmatsci. 2017.07.004
20. Jiang S, Li Q, Wang J, He Z, Zhao Y, Kang M (2016) Multiscale graphene oxide-carbon fiber reinforcements for advanced polyurethane composites. Compos Part A Appl Sci Manuf 87:1–9. https://doi.org/10.1016/j.compositesa.2016.0 4.004
21. Jang BZ, Zhamu A (2008) Processing of nanographene platelets (NGPs) and NGP nanocomposites: a review. J Mater Sci 43(15):5092–5101. https://doi.org/10.1007/s10 853-008-2755-2
22. Hamori H, Kumazawa H, Higuchi R, Yokozeki T (2020) Gas permeability of CFRP cross-ply laminates with thin-ply barrier layers under cryogenic and biaxial loading conditions. Compos Struct 245,112326:1–7
23. Raine TP, Istrate OM, King BE, Craster B, Kinloch IA, Budd PM (2018) Graphene/polyamide laminates for supercritical CO2 and H2S barrier applications: an approach toward permeation shutdown. Adv Mater Interfaces 5(15),1800304:1–6.
24. Pavan, G., Singh, K. K., & Mahesh. (2021). Elevated thermal conditioning effect on flexural strength of GFRP laminates: An experimental and statistical approach. Materials Today Communications, 26, 101809.
25. Rodríguez-García, V., Gómez, J., Cristiano, F., & Gude, M. R. (2020). Industrial manufacturing and characterization of multiscale CFRP laminates made from prepregs containing graphene-related materials. Materials Research Express, 7(7), 075601. doi:10.1088/2053-1591/aba0eb